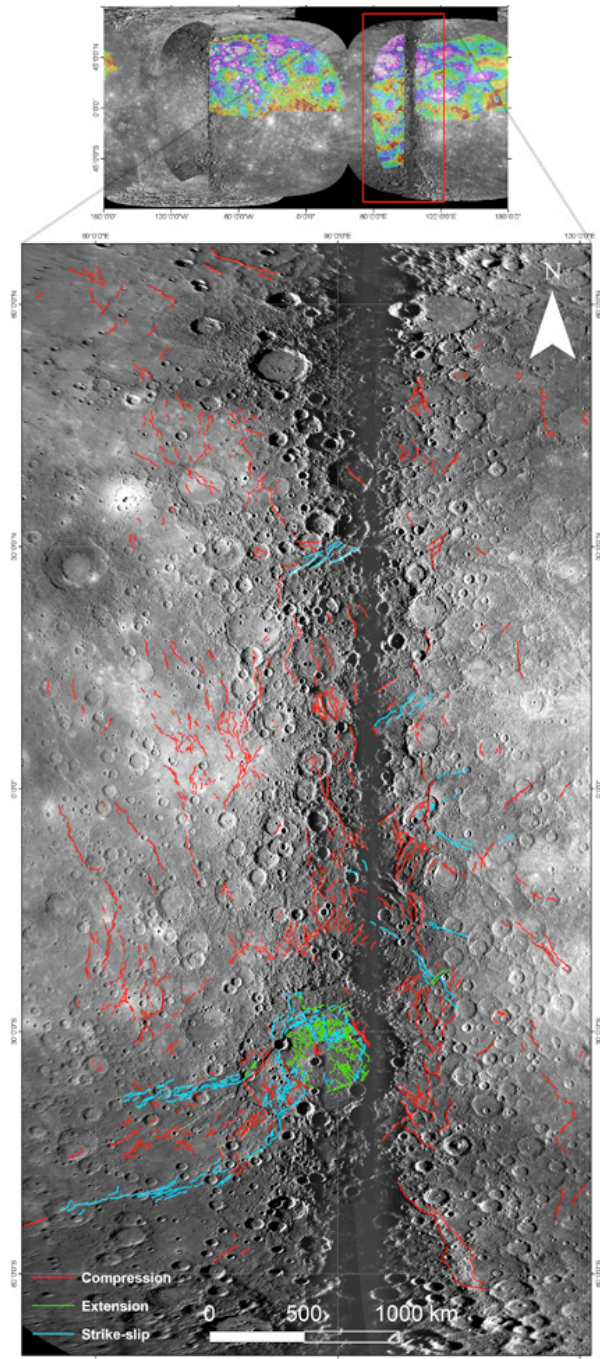


**MAPPING MERCURY'S TECTONIC FEATURES AT THE TERMINATOR: IMPLICATIONS FOR RADIUS CHANGE ESTIMATES AND THERMAL HISTORY MODELS.** G. Di Achille<sup>1</sup>, C. Popa<sup>1</sup>, M. Massironi<sup>2</sup>, S. Ferrari<sup>2</sup>, L. Giacomini<sup>2</sup>, E. Mazzotta Epifani<sup>1</sup>, R. Pozzobon<sup>2</sup>, M. Zusi<sup>1</sup>, G. Cremonese<sup>3</sup>, P. Palumbo<sup>4</sup>, <sup>1</sup>Istituto Nazionale di Astrofisica, Osservatorio Astronomico di Capodimonte, Napoli, Italy, <sup>2</sup>Dipartimento di Geoscienze, Università degli Studi di Padova, Italy, <sup>3</sup>Istituto Nazionale di Astrofisica, Osservatorio Astronomico di Padova, Italy, <sup>4</sup>Dipartimento di Scienze Applicate, Università Parthenope, Napoli, Italy,.

**Introduction:** Prior to the MESSENGER mission [1] only 45% of the Mercury's surface was imaged by Mariner 10 [2]. By using the latter data for mapping tectonic features it was suggested that the detected compressional structures can account for a planetary radius contraction of less than 1 km (0.43-0.64 km) [3-8]. These results have been slightly revised by recent studies using images acquired during the three MESSENGER flybys [7,8]. In fact, several previously unobserved compressional features (including the longest known to date on Mercury) have been discovered [7], increasing the total number of known contractional features by approximately one third and thus bringing the amount of estimated radius contraction to 0.8 km [7,8]. However, these estimates yet appear too low with respect to the amount of radius contraction (up to 5-6 km) predicted by the most accredited studies based on thermo-mechanical evolution models [9-12].

**Motivation:** As already cautioned by previous studies, the identification of tectonic features on Mercury might be largely biased by the lighting geometry of the used basemaps. This limitation might have affected the results of the extrapolations for estimating the radius change [e.g. 5,7,8]. We mapped tectonic features at the terminator thus using images acquired at high sun incidence angle which represents the optimal condition for their observation. This favorable illumination conditions allowed us to infer reliable measurements of spatial distribution (i.e. frequency, orientation, and areal density) of tectonic features which can be used to estimate the average contractional strain and planetary radius decrease.

**Data and methods:** We used all the publicly released data available through the Planetary Data System archive. These include images obtained by Mariner 10 and by the MDIS camera [13] during the MESSENGER flybys and the first two months of orbital operations, and digital terrain models (DTMs) derived from stereo images acquired by the MESSENGER spacecraft's three Mercury flybys [14]. Particularly, we processed the data through the USGS ISIS3 software and integrated all the map projected products into a Geographic Information System (GIS) database. We focused on the terminator area (Figure 1) and used images at high sun incidence angle



**Figure 1.** (top) Global map of Mercury with color-coded topography from [14] and location (red rectangle) of the mapped area shown in the enlarged view

(>50°) to digitize tectonic structures within a region extending for an area of about  $1.20 \times 10^7$  sq. km (~16% of planet's surface). Subsequently, using the approach described in detail in [3,7,8] and based on the displacement-length relationship of tectonic features, we estimated the amount of areal strain accommodated by the compressional structures considering fault dip angles for lobate scarps ranging from 25° to 35° and corresponding  $\gamma$  values ranging from  $6.0\text{--}8.1 \times 10^{-3}$  (with  $\gamma=6.9 \times 10^{-3}$  for  $\theta=30^\circ$ ) [8], while we used  $\gamma=3.5 \times 10^{-3}$  and  $\theta=30^\circ$  for wrinkle ridges. Finally, assuming that the contractional strain recorded within the survey area reflects the average tectonism due to the planet's contraction we extrapolated the results to estimate the amount of radius decrease.

**Results and discussion:** More than 1300 tectonic lineaments were identified and interpreted to be compressional features (i.e. lobate scarps, wrinkle ridges, and high relief ridges) with a total length of more than 12300 km (Figure 1). Moreover, we found that approximately one fourth of these structures (light blue features mapped in Figure 1) most likely have also had significant strike-slip kinematic components [15]. Whereas, extensional features (green features mapped in Figure 1) within the area seem to be exclusively associated to the interior smooth plains of the Rembrandt impact basin. Additionally, although more robust statistical analyses are still underway, the tectonic lineaments appear to be uniformly distributed within the mapped area as would be expected if they were produced in response to an isotropic process.

Table 1 summarizes our results. Assuming that the extensional strain is negligible within the area, the average contractional strain calculated for the survey area is ~0.21–0.28% (~0.24% for  $\theta=30^\circ$ ). This strain, extrapolated to the entire surface, corresponds to a contraction in radius of about 2.5–3.4 km (~2.9 km for  $\theta=30^\circ$ ) lowered to 2.2–3.0 km (~2.6 km for  $\theta=30^\circ$ ) when considering the transcurrent faults with pure strike-slip component and thus not contributing to the total contractional strain. Actually, it would be more reasonable to assume intermediate figures between the above radius changes. In fact, it is more likely that the transcurrent segments of the faults accommodated some amount of contractional strain as well, i.e. they

**Table 1** - Summary of results. Radius changes within brackets were obtained considering pure strike-slip components for transcurrent faults (see text for details)

Fault dip angle (deg.)	25	30	35
Strain (%)	0.28	0.24	0.21
Radius decrease (km)	3.4 (3.0)	2.9 (2.6)	2.5 (2.2)

acted as transpressional features.

Interestingly, the values of contractional strain and radius decrease obtained in the present study are from four to five times higher with respect to previous estimates [3-8]. Indeed, although the total amount of contraction is still debated [9-12], recent estimates suggest that the Mercury's radius contraction could have been up to 5-6 km throughout its thermal evolution [11,12]. Additionally, lower values of radial contraction (1-2 km) would be possible only with restricted ranges of planet bulk composition and rheology [11,12]. For this reason, it has been suggested that there may be hidden strain accommodated by features yet unseen on Mercury [11,12]. Our results are more compatible with the latter predictions than previous results [e. g. 3-8], supporting the idea that Mercury could have recorded more tectonism than that required to account for 1-2 km of radial contraction and thus enabling the test of alternative compositional and/or cooling models with respect to those constrained exclusively by the lower bounds for radius decrease.

Our results are particularly reliable since we used images with optimum sun incidence angle for mapping tectonic features. Nonetheless, these estimates should be confirmed by further observations over significant portions of the planet and at most favorable sun angle conditions using data from the MESSENGER orbital phase and the high resolution basemaps which will be provided by the next BepiColombo mission [e. g. 16]. Finally, the present study suggests that strike-slip faults are likely more widespread than previously thought [15] and that it is important to assess the role played by this kinematic component since it might affect estimates of strain up to more than ten percent.

**References:** [1] Solomon S. C. et al. (2008) *Science*, 321, 59. [2] B. C. Murray (1975) *JGR*, 80, 2342. [3] Watters T. R. et al. (1998) *Geology*, 26, 991–994. [4] Watters T.R. et al. (2001) *Planet. Space Sci.*, 49, 1523–1530. [5] Watters T. R. et al. (2004) *GRL*, 31, L04701. [6] Watters T.R. et al. (2000) *GRL*, 27, 3659–3662. [7] Watter T.R. et al. (2009) *Earth Planet. Sci. Lett.*, 131, 247. [8] Watters T. R. and Nimmo F. (2010) in *Planetary Tectonics*, Cambridge University Press. [9] Solomon S. C. (1976) *Icarus*, 28, 509–521. [10] Schubert G. et al. (1988) in *Mercury*, University of Arizona Press. [11] Hauck S. A. et al. (2004) *Earth Planet. Sci. Lett.*, 222, 713–728. [12] Dombard A. J and Hauck S. A. (2008) *Icarus*, 198, 274–276. [13] Hawkins S. E. III et al. (2007) *Space Sci. Rev.*, 131, 247. [14] Preusker F. et al. (2009) *Planet. Space Sci.*, 59(15), 1910–1917. [15] Massironi M. et al. *this issue*. [16] Flamini E. et al. (2010) *Planet. Space Sci.*, 58, 116.